Tubulin-based Structure-affinity Relationships for Antimitotic *Vinca* Alkaloids

Claire Coderch[1], Antonio Morreale[2] and Federico Gago[1,#,*]

[1]*Departmento de Farmacología, Universidad de Alcalá, 28871 Alcalá de Henares, Madrid, Spain;* [2]*Unidad de Bioinformática, Centro de Biología Molecular Severo Ochoa (CSIC, UAM), Campus Cantoblanco, 28049 Madrid, Spain*

Abstract: The *Vinca* alkaloids are a group of widely used anticancer drugs, originally extracted from the Madagascar periwinkle, that disrupt microtubule dynamics in mammalian cells by interfering with proper assembly of α,β-tubulin heterodimers. They favor curved tubulin assemblies that destabilize microtubules and induce formation of spiral aggregates. Their binding energy profiles have been characterized by means of sedimentation velocity assays and the binding site of vinblastine at the interface between two tubulin dimers ($\alpha_1\beta_1$–$\alpha_2\beta_2$) has been ascertained by X-ray crystallographic studies on a complex of tubulin with the stathmin-like domain of protein RB3, albeit at relatively low resolution. Here we use molecular modeling and simulation techniques to build, refine and perform a comparative analysis of the three-dimensional complexes of vinblastine, vincristine, vinorelbine and vinflunine with a $\beta_1\alpha_2$-tubulin interface in explicit water to rationalize the binding affinity differences in structural and energetic terms. Our results shed some more light into the binding determinants and the structure-activity relationships of these clinically useful agents.

Keywords: Tubulin, Antimitotic drugs, *Vinca* alkaloids, Computer simulations, Binding energy analysis, Molecular dynamics.

[#]**Author Profile:** Federico Gago studied Pharmacy at Complutense University, Madrid, and followed post-doctoral studies at the Physical Chemistry Laboratory, Oxford University. He is currently a Full Professor in the Department of Pharmacology at the University of Alcalá, near Madrid, where he pursues research work in the areas of computer simulations of biomolecular systems and structure-based drug design.

INTRODUCTION

Microtubules (MT) are key cell structures found in eukaryotes that play a vital role in the organization of the spatial distribution of organelles throughout interphase and of chromosomes during cell division. MT assemble from protofilaments built through longitudinal head-to-tail juxtaposition of α,β-tubulin heterodimers. α- and β-tubulin are the most conserved proteins in eukaryotes and they belong, along with their prokaryotic ancestors, to the distinct tubulin superfamily of GTPases, whose common structure is an N-terminal, or nucleotide binding domain, connected by a core helix (H7) to a C-terminal domain [1]. Each monomer binds a GTP molecule [2] but, whereas the nucleotide bound to the α subunit is nonhydrolysable and nonexchangeable, that bound to the β subunit is hydrolysable and exchangeable in unassembled tubulin heterodimers. This is so because, upon head-to-tail assembly of two heterodimers, residues from the α subunit complete the functional architecture of the GTP hydrolysis site in the β subunit. Subsequently, once the γ-phosphate group has been cleaved, GDP is sequestered at the nucleotide exchangeable site and MT disassemble by peeling outwards. Catastrophe ensues when the disassembly rate dominates over assembly formation and this occurs because the once straight GTP-bound tubulin heterodimers curve following hydrolysis of the GTP nucleotide [3]. Since GTP hydrolysis accompanies MT assembly, and GDP-tubulin is released upon depolymerization, tubulin has to exchange its bound GDP with GTP in order to assemble again. These two properties, GTP hydrolysis and nucleotide exchange, are therefore intrinsic to tubulin. MT dynamics is also affected by the presence of the cell-cycle regulating protein stathmin, which interacts with two α,β-tubulin heterodimers to form a tight ternary complex, the so-called T2S complex, that is unsuitable for MT formation. Stathmin phosphorylation on Ser16, Ser25, Ser38 and Ser63 by cell cycle kinases at the onset of mitosis weakens this association and the increased concentration of tubulin available in the cytoplasm allows the assembly of the mitotic spindle [4]. Another regulatory mechanism in cell proliferation is the alteration of the rate of catastrophe brought about by the existence of different β-tubulin isotypes [5, 6]. Moreover, recent evidence has demonstrated the presence of unhydrolysed GTP-bound tubulin not only at the growing end of MT but also in older parts where it could play a role in the rescue events that recover these structures from catastrophe [7].

MT dynamics, and therefore cell division, can also be perturbed by small molecules, and this interference can lead to cell death [8]. This antimitotic property is, in fact, exploited by a number of potent anticancer chemotherapeutic drugs, which are usually divided into two groups: (i) MT-stabilizing agents that prevent depolymerization, and (ii) MT-depolymerizing agents that inhibit MT formation. The former bind to polymerized MT, stabilize the M-loop that is responsible for lateral interactions between neighboring protofilaments, and prevent depolymerization even after GTP hydrolysis [9]. A common characteristic of these drugs is that they have two binding sites: an external site of lower affinity located at the MT pore to which they bind before being internalized to the lumen, and a higher-affinity luminal site located inside the MT [10-12]. The best known MT-stabilizing drugs are the clinically used taxanes, paclitaxel (Taxol®) and docetaxel (Taxotere®) [13], and the epothilone B analogue ixabepilone (IXEMPRA®) [14].

MT-destabilizing agents bind to unpolymerized tubulin and block MT formation. Two distinct binding sites were early recognized, with affinities for colchicine and the so-called *Vinca* alkaloids, respectively. Colchicine is a secondary metabolite produced by plants of the genus *Colchicum* that has been known for centuries for its pain-relieving effects in acute gout flares and has also been used to induce polyploidy in plant cells because it inhibits chromosome segregation during meiosis. Vinblastine (a.k.a. vincaleukoblastine, VLB) and vincristine (VNC), on the other hand, were originally isolated from the Madagascar periwinkle (*Catharanthus roseus*, basionym *Vinca rosea*) and have been in clinical use for the chemotherapy of a number of hematological and solid tumors for many years [15]. The capacity of these alkaloids to arrest cells in metaphase is due to the fact that they inhibit the assembly and dynamics of MT.

*Address correspondence to this author at the Departmento de Farmacología, Universidad de Alcalá, 28871 Alcalá de Henares, Madrid, Spain;
Tel: +34-918854514; Fax: +34-918854591;
E-mail: federico.gago@uah.es

1875-5992/12 $58.00+.00 © 2012 Bentham Science Publishers

The colchicine-binding site is a pocket located within β-tubulin at the interface with the α-subunit of the same heterodimer [16]. Addition of colchicine to steady-state MT inhibits their growth and induces their disassembly into heterodimers [17]. Several crystal structures (Protein Data Bank [PDB] entries 1SA0, 1SA1, 3HKC, 3HKD, 3HKE, 3N2K, and 3N2G) have been solved of protein complexes comprising the stathmin-like domain of protein RB3 (RB-SLD) and two tubulin heterodimers with ligands bound at the colchicine-binding site. These complexes show a curved arrangement of tubulin that prevents it from adopting the straight conformation needed for MT formation [18]. Soaking of some of these crystals with VLB [19] and use of synchroton radiation allowed Knossow *et al.* to determine the binding site for this alkaloid at 4.1 Å resolution: VLB is located at the longitudinal interface between two tubulin heterodimers next to the exchangeable GTP-binding site (E-site) [20]. This location explains why the *Vinca* alkaloids inhibit GTP hydrolysis [21], a bimolecular process in which residues from the α-tubulin subunit are used to catalyze the cleavage of the β-γ phosphodiester linkage of the GTP molecule bound to the neighboring β-tubulin subunit. The observed bent structure also accounts for the tendency of these drugs to induce self-association of tubulin into spiral aggregates at the expense of MT growth [22]. Interestingly, a bent conformation of free tubulin dimers has recently been demonstrated, which suggests that stathmin evolved to recognize curved structures in unassembled and disassembling tubulin [23].

Since the binding of natural *Vinca* alkaloids, as well as that of their semi-synthetic analogs vinorelbine (VNR) and vinflunine (VFN)[24], is linked to tubulin self-association, their affinities have been determined by sedimentation velocity experiments at different temperatures. These studies have concluded that their binding is entropically driven and that the overall affinities decrease in the order VNC > VLB > VNR > VFN, with the latter inducing the shortest spirals [25-27]. However, the affinity of the four compounds for tubulin heterodimers appears to be almost identical, the major differences among them being due to the distinct affinities of the resulting liganded heterodimers for polymerized spirals. Likewise, no preference for binding to certain tubulin isotypes over others has been observed although the binding was reported to be enhanced by the presence of GDP rather that GTP in the nucleotide binding site [28]. On the other hand, the origin of the positive binding enthalpy (ΔH) and/or the contributions to the observed enthalpy-entropy (ΔS) compensations [29, 30] remain to be established.

The binding of VLB to tubulin can be inhibited non-competitively by yet another class of compounds represented by halichondrin B, which was first extracted from a marine Japanese sponge, *Halichondria okadai* [31], and by its synthetic analogue, eribulin, which is approved for the treatment of metastatic breast cancer [32]. These agents bind to β-tubulin near the exchangeable GTP-binding site [33] but do not affect the binding of colchicine [34]. They suppress MT growth and sequester tubulin into nonfunctional aggregates [35] but, unlike the *Vinca* alkaloids, they have no effect on MT shortening.

In this study we have tried to shed some more light into the binding of VLB, VNC, VNR and VFN (Fig. **1**) to tubulin heterodimers using molecular modeling techniques, molecular dynamics (MD) simulations, continuum electrostatics calculations and energy decomposition analysis.

METHODOLOGY

The crystal structure of the VLB-colchicine-tubulin-RB-SLD assembly at 4.1 Å resolution (PDB entry 1Z2B) was used as a template to build molecular models of the whole set of complexes. For computational limitations, our systems comprised the GDP-bound β-tubulin subunit of the "bottom" heterodimer (β_1), the GTP-Mg^{2+}-bound α-tubulin subunit of the "top" heterodimer (α_2) and the respective *Vinca* alkaloid bound at the interface between them (Fig. **2**). VNC, VNR and VFN were modeled inside the binding site by editing and refining the three-dimensional structure of VLB. The molecular graphics program PyMOL version 0.99 (DeLano Scientific, LLC, Palo Alto, CA) was employed for visualization and model building.

Addition of missing hydrogen atoms and computation of the protonation state of titratable groups in α and β-tubulin at pH 6.5 were carried out using the H++ Web server [36], which relies on AMBER [37] force-field parameters and finite difference solutions

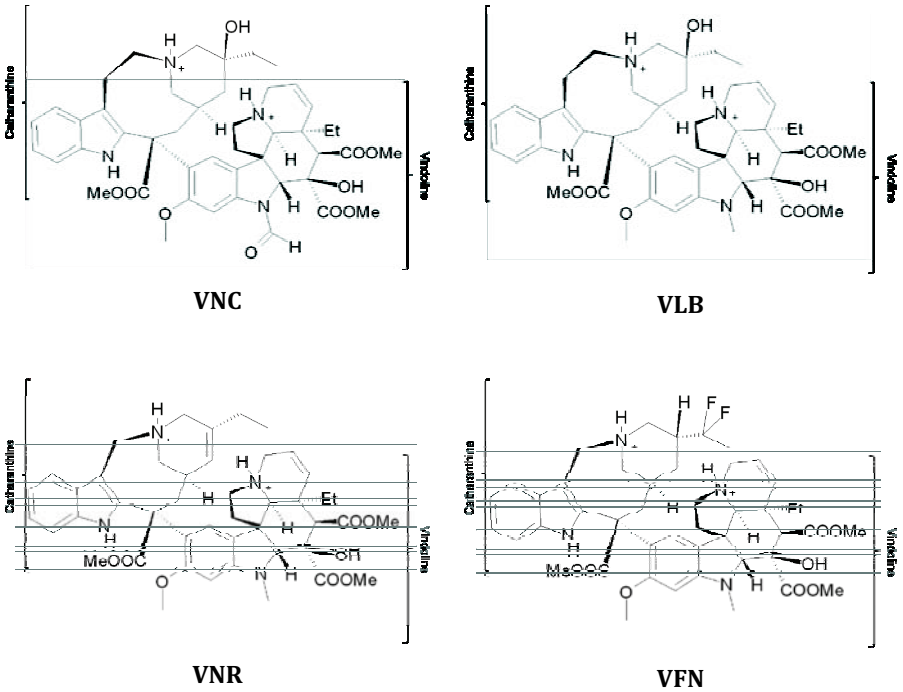

Fig. (1). Chemical formulae of the four *Vinca* alkaloids studied: vinblastine (VLB), vincristine (VNC), vinorelbine (VNR) and vinflunine (VFN).

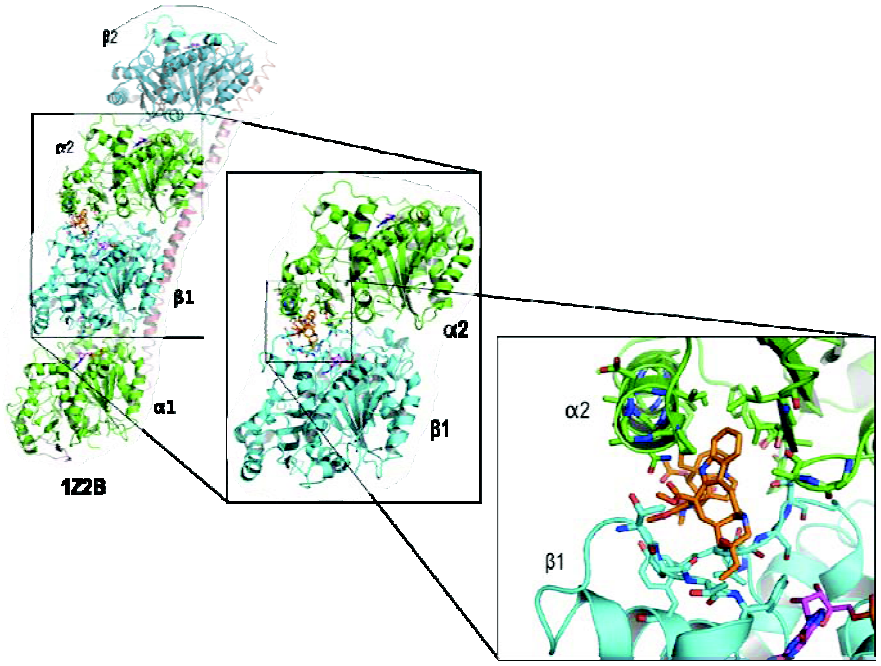

Fig. (2). PyMOL representation of the two αβ-tubulin heterodimers (α-tubulin in green, β-tubulin in cyan, and GTP and GDP nucleotides in magenta) stabilized by colchicine (represented in grey sticks) and bound to VLB (represented as orange sticks) and the stathmin-like domain of protein RB3 (pink helix), as found in PDB entry 1Z2B. The central figure represents the system that was extracted and solvated for our simulations.

to the Poisson-Boltzmann equation [38]. The charge distribution for the ligands studied was obtained by fitting the quantum mechanically calculated (RHF/6-31G*//RHF/3-21G*) molecular electrostatic potential (MEP) of the geometry-optimized molecule to a point charge model, as implemented in Gaussian 03 (Gaussian, Inc., Wallingford, CT). Consistent bonded and non-bonded AMBER parameters for the *Vinca* alkaloids were assigned by analogy or through interpolation from those already present in the AMBER database (ff03). Each molecular system was immersed in a truncated octahedron containing ~32,300 TIP3P water molecules [39] and 23 Na^+ ions [40] to achieve system electroneutrality. The *sander* and *pmemd* modules from the AMBER10 suite (http://ambermd.org/) were used for the restrained and unrestrained MD simulations, respectively. Periodic boundary conditions were applied and electrostatic interactions were treated using the smooth particle mesh Ewald method [41] with a grid spacing of 1 Å. The cutoff distance for the non-bonded interactions was 9 Å, the SHAKE [42] algorithm was applied to all bonds, and an integration step of 2.0 fs was used throughout. After an initial energy minimization of the water molecules and counterions, the system was heated to 300 K in 25 ps after which the solvent was allowed to redistribute around the positionally restrained solute for 220 ps. After this time, only the protein Cα atoms were restrained with a harmonic force constant of 10 kcal/mol·Å^2 so as to explore the mutual adaptation between ligand and amino acid side chains without altering the overall conformation of the dimer. Snapshots from each 10-ns MD trajectory were collected every 20 ps for further analysis. For visualization purposes, a representative average structure for each complex was calculated and refined using energy minimization.

To get an estimate of the free energy change that describes tubulin-ligand binding we calculated the difference between the free energy of the complex and that of the respective binding partners using a hybrid molecular mechanics (MM)/generalized Born-surface area (GBSA) approach, as implemented in AMBER 10 [43, 44]. Energy values were calculated as the averages over 200 snapshots from the middle part of the production phase of the MD trajectory for each complex. The van der Waals contribution to the binding energy was represented as the sum of the total ΔG_{vdW} calculated in the gas phase and the total ΔG_{surf} calculated from the solvent-accessible surface area (SASA) [45], which was determined using a water probe of radius 1.4 Å. The electrostatic contribution to the binding energy was estimated as the sum of the total ΔG_{ele} calculated in the gas phase and the total ΔG_{GB} calculated by solving the generalized Born equation [46] using dielectric constants of 1 and 78.5 for solute and solvent, respectively.

To study the conformational space of free VLB in aqueous solution, the drug was extracted from the complex and, in its bound conformation, immersed in a cubic box containing ~1,400 TIP3P water molecules and a chloride ion to achieve electroneutrality. The energy of this system was minimized in the AMBER force field prior to running unrestrained MD simulations for 100 ns using the same conditions as for the complexes. The trajectories were then processed with the *ptraj* module in the AMBER 11 suite to estimate the root-mean-square deviation (RMSD) from the bound initial geometry and to cluster the resulting conformers of the drug in bulk solvent. The relative energies of each conformer were extracted and used to calculate the probability of the microstates as defined by the Boltzmann distribution formula:

$$p_i = n\, e^{-Ei/RT} / \Sigma_j\, n\, e^{-Ei/RT}$$

where n is the number of structures belonging to each cluster i, E_i is the energy of the average structure extracted from i, T is the temperature in Kelvin, R is the gas constant expressed in kcal/mol, and j is the total number of clusters.

RESULTS AND DISCUSSION

The 100-ns MD simulation of VLB in aqueous solution provided conformations that did not differ from the initial structure by more than 1.5 Å of RMSD. The clustering analysis identified three main conformers differing in just the value of the torsional angle relating the catharanthine and vindoline domains. The most populated one, by far, was precisely that found in the complex with tubulin in the crystal structure. Thus, we can state that the VLB structure, and by extension that of the other *Vinca* alkaloids, is quite rigid and that the conformation of the ligand in aqueous solution is likely to be the same as that present in the VLB-tubulin complex (Fig. **3**). Therefore we can safely assume that these compounds are

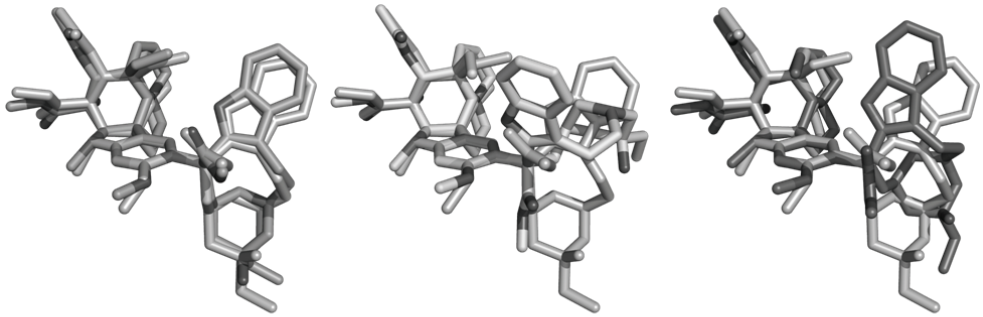

Fig. (3). Best-fit superposition of the three conformers of VLB extracted from the MD simulation in aqueous solution over the initial tubulin-bound structure (light gray). The ratio between relative energy of the conformer (E_r) and the probability of the microstate according to the Boltzmann distribution (p_i) is shown.

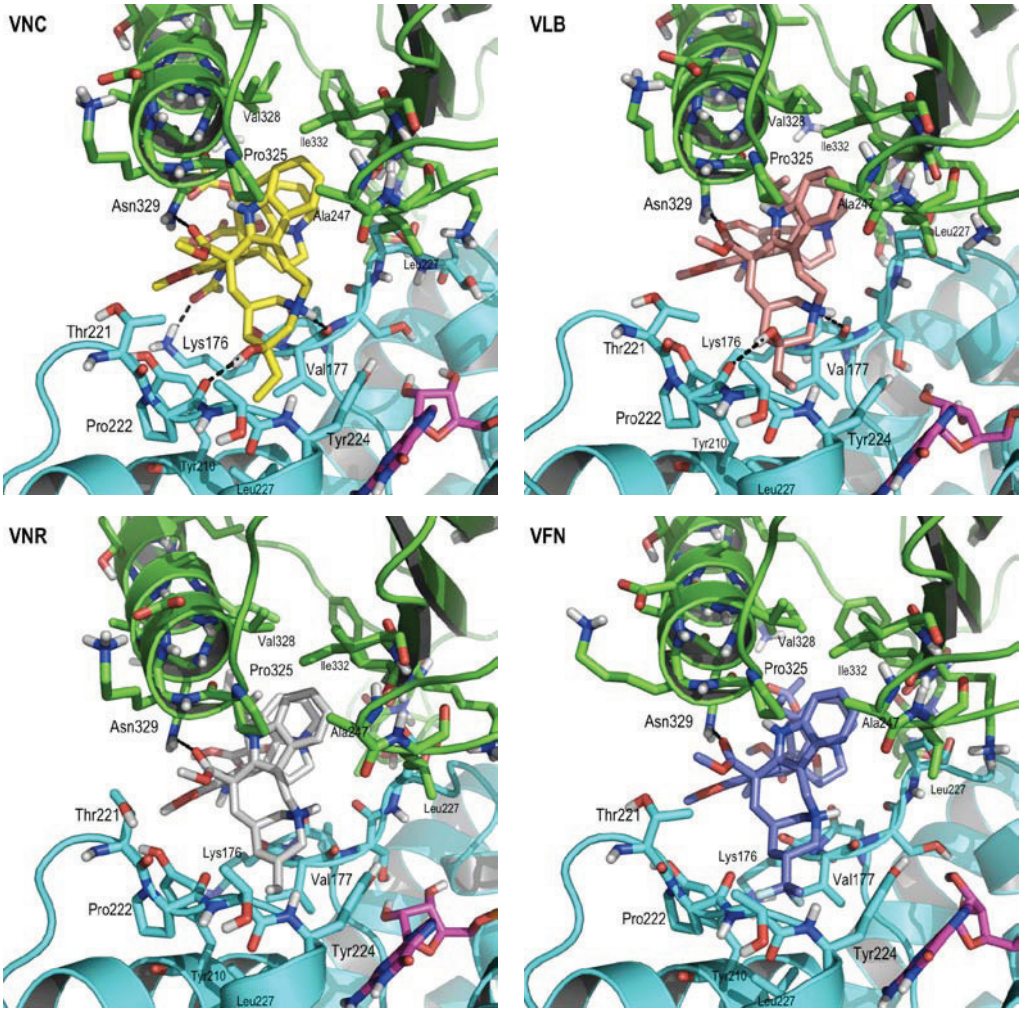

Fig. (4). Detail of the drug-binding site at the $\beta_1\alpha_2$-tubulin (cyan/green) interface in each of the complexes studied after the MD simulation and subsequent energy refinement of the average structure. VNC (yellow), VLB (pink), VNR (white), VFN (blue), and GDP (magenta) are shown as sticks as well as the amino acids charted in the energy decomposition analyses. Only polar hydrogens are displayed and hydrogen-bonding interactions are depicted as broken lines. For clarity only the main drug-interacting amino acids have been labeled.

highly preorganized for binding to curved tubulin at the $\beta_1\alpha_2$ interface between heterodimers.

In their respective complexes with $\alpha_2\beta_1$-tubulin, mutual adaptation during the MD simulations between the drugs and the side chains of the amino acids making up the binding site improved the intermolecular interactions and provided distinct details for each complex. The four *Vinca* alkaloids studied (Fig. **1**) exhibit overall similar van der Waals and electrostatic interaction energy terms (Fig. **4**) thereby defining a common pharmacophore. Their binding site is lined by the side chains of a number of mostly non-polar amino acids from both tubulin monomers. Thus, in the β subunit, $Val_{\beta1}177$, $Tyr_{\beta1}210$, $Thr_{\beta1}221$, $Pro_{\beta1}222$, $Thr_{\beta1}223$, $Tyr_{\beta1}224$ and $Leu_{\beta1}227$ are in close contact with the catharanthine domain whereas $Pro_{\beta1}175$ and $Lys_{\beta1}176$ provide an interacting surface for the vindoline domain. In the α subunit, the side chains of $Leu_{\alpha2}248$ and $Pro_{\alpha2}325$ establish contacts mainly with the indole ring in

the catharanthine domain while $Val_{\alpha 2}328$, $Asn_{\alpha 2}329$, $Ile_{\alpha 2}332$, $Ala_{\alpha 2}333$, and $Val_{\alpha 2}353$ interact with both drug domains. There are two common intermolecular hydrogen bonding interactions: one between the carboxamide of $Asn_{\alpha 2}329$ and the methyl-ester in the catharanthine domain, and another between the charged amino group in the catharanthine domain and the backbone carbonyl of $Val_{\beta 1}177$. But while this latter interaction is a direct hydrogen bond in the complexes with VNC and VLB, the slight change of geometry induced by the shortening by one carbon of the seven-member ring in the catharanthine domain of VNR and VFN causes this interaction to be water-mediated, which could be translated into a lower affinity. Importantly, the formyl group on the indole ring of VNC that replaces the methyl in VLB is able to engage in a hydrogen-bonding interaction with the positively charged amino group of $Lys_{\beta 1}176$. This must be relevant for the *in vivo* action of these two drugs because VNC and VLB, despite this minor structural variation, are endowed with distinct spectra of pharmacological activity and dose-related toxicities, as well as differential cellular uptake and retention characteristics [47, 48].

The binding features of the four structurally similar analogs can be compared pairwise because the differences among them are mostly confined to the number of carbon atoms in the central saturated ring of the catharanthine domain and the presence or absence of a hydroxyl group in the common six-membered ring of this same domain. Thus, VNR and VFN lack the hydroxyl in their six-membered ring (Fig. **1**) whereas VNC and VLB have a seven-membered ring with an attached hydroxyl that acts as a hydrogen bond donor to the carbonyl oxygen of $Pro_{\beta 1}222$. On the other hand, the saturated double bond and the two fluorine atoms that differentiate VFN from VNR provide only a marginally improved electrostatic interaction with $Val_{\beta 1}177$ and $Tyr_{\beta 1}224$ (Fig. **5**). Taken together, our results are therefore in overall semiquantitative agreement with the binding affinities measured experimentally (VNC> VLB > VNR > VFN).

It must be realized that in curved tubulin the binding site we have studied is exposed to the solvent and displacement of any bound water molecules by drug binding must be accompanied by the release of these water molecules into the bulk solvent, which is thought to result in a significant entropic contribution to the binding energy. The same can be said about the water molecules in contact with the hydrophobic surfaces of the drugs that are released upon complex formation. These two processes are likely to underlie the experimental observation that binding of these drugs to tubulin is an entropically driven process [25, 26, 49]. For the better studied HIV protease, it was concluded for some ligands that the origin of an unfavorable enthalpy, despite the fact that intrinsic interactions were favorable, was the energy cost of rearranging the flap region in the enzyme and that the dominant binding force was the increase in solvent entropy that accompanies the burial of a significant hydrophobic surface [30].

One limitation of our first approximation to the binding of these agents to tubulin is, of course, the restraints that we imposed on the Cα trace of the protein. This was done to prevent any major artifactual distortions on tubulin in the absence of protein RB3, which was not included in our simulations for computational efficiency. This limitation may have prevented a deeper burial of both VNR and VFN in the binding site so as to establish a direct hydrogen bond between the charged amino group in the catharanthine domain and the backbone carbonyl of $Val_{\beta 1}177$. If this were the case, the wedge effect at the $\beta_1\alpha_2$-tubulin interface upon drug binding would be greater for VNR and VFN than that observed for VLB and VNC, and this may well account for the finding that the spiraling potential of VFN, a property that happens to be inversely related to the clinically used dosage, is the lowest of all [25, 50].

Since it is well known that MT's behavior depends on β-tubulin isotype composition [5], one could have expected differential interactions between these drugs and tubulins of diverse amino acid composition at both the inter-dimer and intra-dimer interfaces [6]. However, when we performed a multiple sequence alignment (Fig. **6**) and mapped the drug pharmacophoric region onto it no differences were found. Therefore, and taking into account that these alkaloids bind to unpolymerized curved tubulin, their different

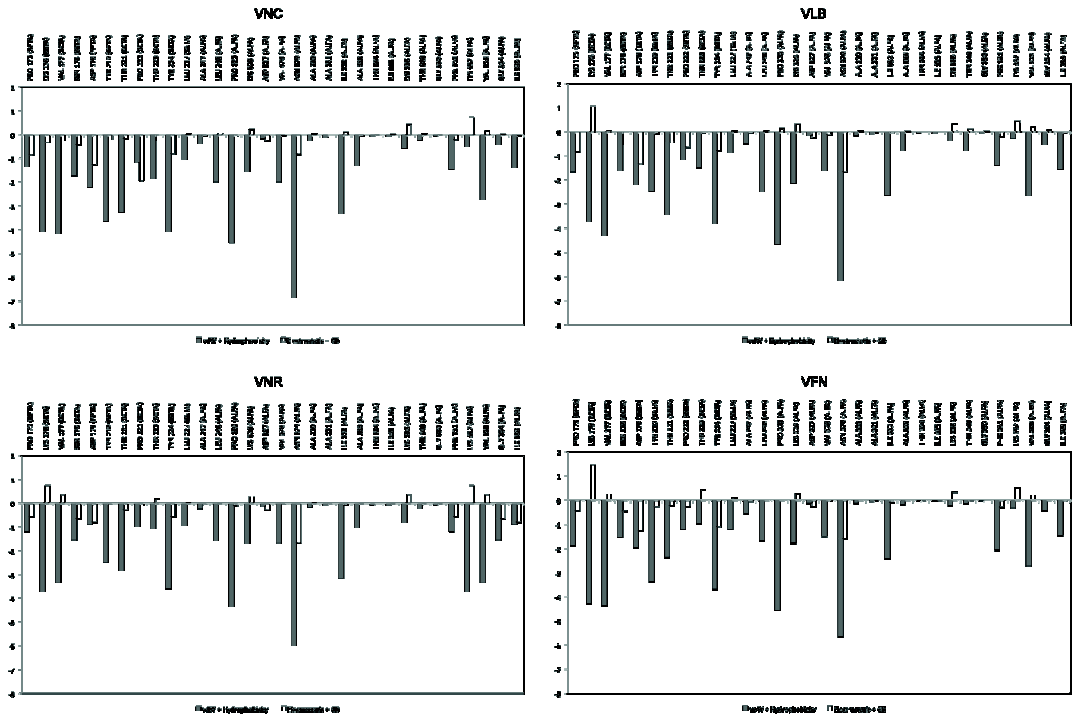

Fig. (5). Residue-based free energy decomposition for the binding of the four *Vinca* alkaloids to the $\beta_1\alpha_2$-tubulin interface. The filled bars represent van der Waals energy + hydrophobicity (SASA) while the empty bars stand for the sum of electrostatic (ΔG_{ele} in the gas phase) and desolvation (total ΔG_{GB}) energies.

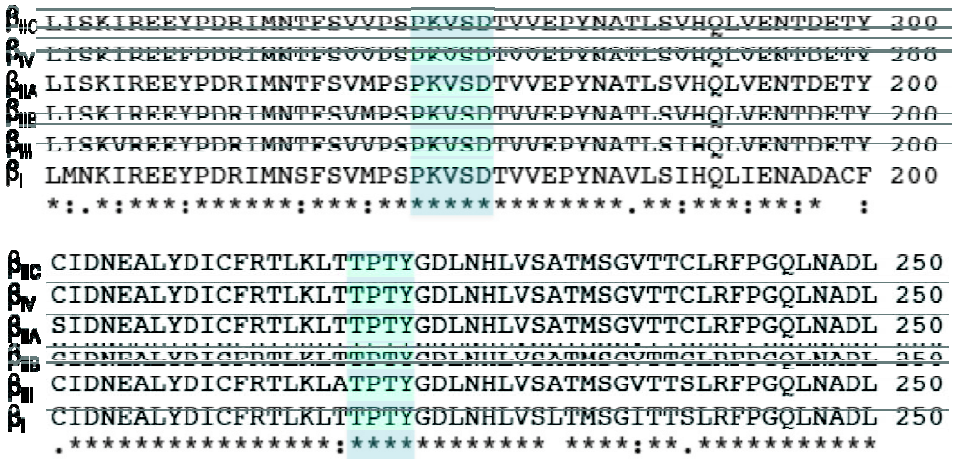

Fig. (6). Multiple sequence alignment of the β-tubulin isotypes β_I (Q9H4B7), β_{IIA} (Q13885), β_{IIB} (Q9BVA1), β_{IIC} (P68371), β_{III} (Q13509) and βIV (P04350). The shaded boxes highlight the β-tubulin regions that interact with the *Vinca* alkaloids, which happen to be of identical sequence in all isotypes. Asterisks, colons, dots and blanks indicate, respectively, identical residues and conservative, semi-conservative, or non-conservative mutations.

binding affinities must surely arise from distinct kinetics of MT formation and catastrophe being exhibited by the tubulin isotypes and their mixtures rather than from changes in drug-protein interaction patterns.

CONCLUSIONS

An MD simulation of VLB in aqueous solution showed a conformational rigidity in this alkaloid that is translated into a high degree of preorganization for tubulin binding and can be safely assumed for the remaining members of the *Vinca* family of drugs. By extracting the relevant interdimer interface from the only available crystal structure of VLB-bound tubulin and using model building and simulation techniques, we explored the conformational behavior of the drug-binding site in the presence of VLB, VNC, VNR and VFN. The resulting complexes showed a distinct and consistent pattern of intermolecular interactions that were analyzed using the MM/GBSA approach. An extensive number of van der Waals contacts and a number of hydrogen-bonding interactions were apparent that nevertheless could not account for the entropy-driven free energy changes measured experimentally [25, 26]. This is probably due to enthalpy-entropy compensations arising from polar group desolvation, structural rearrangement of the binding site, and the burial of hydrophobic surfaces upon ligand binding. Nonetheless, we detected the possibility of an extra hydrogen bonding interaction between VNC and $Lys_{\beta1}176$ that is not possible for VLB and could account for the improved binding energy of the former over the latter and for the distinct biological profiles of these otherwise almost identical drugs [25]. Likewise, the absence in VNR of the interaction involving the hydroxyl group in the catharanthine domain that is present in the other alkaloids might well be responsible for the loss of binding free energy in this derivative compared to VLB [25]. Lastly, it seems that the introduction of the two fluorine atoms in VFN is not translated into an improved thermodynamic profile, in agreement with experimental data showing a worse binding enthalpy for this derivative relative to VNR and consequently to VNC and VLB [26]. The resulting pharmacophore for drug binding cannot explain any differences regarding β-tubulin isotypes, given the fact that the residues in contact with the drugs are highly conserved in the tubulin family. Hence, it is more likely that any differences observed result from variations in the kinetics of MT formation and catastrophe rather than from a distinct set of drug-protein interactions.

CONFLICT OF INTEREST

Declared none.

ACKNOWLEDGEMENTS

The authors thankfully acknowledge financial support from Comunidad Autónoma de Madrid (S-BIO/0214/2006) and Comisión Interministerial de Ciencia y Tecnología (SAF2009-13914-C02-02) as well as the computer resources, technical expertise and assistance provided by the Barcelona Supercomputing Center (Centro Nacional de Supercomputación). C.C. enjoys an FPU grant awarded by the Spanish Ministry of Science and Innovation (AP2007-01225). A.M. is grateful to Comunidad Autónoma de Madrid (Consejería de Educación) and Fundación Severo Ochoa for financial support through the AMAROUTO program.

REFERENCES

[1] Nogales, E.; Downing, K.H.; Amos, L.A.; Lowe, J. Tubulin and FtsZ form a distinct family of GTPases. *Nat. Struct. Biol.,* **1998**, *5*, 451-458.

[2] Wade, R.H. Microtubules: an overview. *Methods Mol. Med.,* **2007**, *137*, 1-16.

[3] Nogales, E.; Wang, H.W. Structural intermediates in microtubule assembly and disassembly: how and why? *Curr. Opin. Cell Biol.,* **2006**, *18*, 179-184.

[4] Rubin, C.I.; Atweh, G.F. The role of stathmin in the regulation of the cell cycle. *J. Cell Biochem.,* **2004**, *93*, 242-250.

[5] Panda, D.; Miller, H.P.; Banerjee, A.; Luduena, R.F.; Wilson, L. Microtubule dynamics *in vitro* are regulated by the tubulin isotype composition. *Proc. Natl. Acad. Sci. U S A,* **1994**, *91*, 11358-11362.

[6] Rezania, V.; Azarenko, O.; Jordan, M.A.; Bolterauer, H.; Luduena, R.F.; Huzil, J.T.; Tuszynski, J.A. Microtubule assembly of isotypically purified tubulin and its mixtures. *Biophys. J.,* **2008**, *95*, 1993-2008.

[7] Dimitrov, A.; Quesnoit, M.; Moutel, S.; Cantaloube, I.; Pous, C.; Perez, F. Detection of GTP-tubulin conformation *in vivo* reveals a role for GTP remnants in microtubule rescues. *Science,* **2008**, *322*, 1353-1356.

[8] Jordan, A.; Hadfield, J.A.; Lawrence, N.J.; McGown, A.T. Tubulin as a target for anticancer drugs: agents which interact with the mitotic spindle. *Med. Res. Rev.,* **1998**, *18*, 259-296.

[9] Wade, R.H. On and around microtubules: an overview. *Mol. Biotechnol.,* **2009**, *43*, 177-191.

[10] Buey, R.M.; Calvo, E.; Barasoain, I.; Pineda, O.; Edler, M.C.; Matesanz, R.; Cerezo, G.; Vanderwal, C.D.; Day, B.W.; Sorensen, E.J.; Lopez, J.A.; Andreu, J.M.; Hamel, E.; Diaz, J.F. Cyclostreptin binds covalently to microtubule pores and lumenal taxoid binding sites. *Nat. Chem. Biol.,* **2007**, *3*, 117-125.

[11] Magnani, M.; Maccari, G.; Andreu, J.M.; Diaz, J.F.; Botta, M. Possible binding site for paclitaxel at microtubule pores. *FEBS J.,* **2009**, *276*, 2701-2712.

[12] Barasoain, I.; Garcia-Carril, A.M.; Matesanz, R.; Maccari, G.; Trigili, C.; Mori, M.; Shi, J.Z.; Fang, W.S.; Andreu, J.M.; Botta, M.; Diaz, J.F. Probing the pore drug binding site of microtubules with fluorescent taxanes: evidence of two binding poses. *Chem. Biol.,* **2010**, *17*, 243-253.

[13] Lowe, J.; Li, H.; Downing, K.H.; Nogales, E. Refined structure of alpha beta-tubulin at 3.5 A resolution. *J. Mol. Biol.,* **2001**, *313*, 1045-1057.

[14] Hunt, J.T. Discovery of ixabepilone. *Mol. Cancer Ther.,* **2009**, *8*, 275-281.

[15] Seam, P.; Janik, J.E.; Longo, D.L.; Devita, V.T., Jr. Role of chemotherapy in Hodgkin's lymphoma. *Cancer J.,* **2009**, *15*, 150-154.

[16] Ravelli, R.B.; Gigant, B.; Curmi, P.A.; Jourdain, I.; Lachkar, S.; Sobel, A.; Knossow, M. Insight into tubulin regulation from a complex with colchicine and a stathmin-like domain. *Nature,* **2004**, *428*, 198-202.

[17] Vandecandelaere, A.; Martin, S.R.; Engelborghs, Y. Response of microtubules to the addition of colchicine and tubulin-colchicine: evaluation of models for the interaction of drugs with microtubules. *Biochem. J.,* **1997**, *323 (Pt 1)*, 189-196.

[18] Dorleans, A.; Gigant, B.; Ravelli, R.B.; Mailliet, P.; Mikol, V.; Knossow, M. Variations in the colchicine-binding domain provide insight into the structural switch of tubulin. *Proc. Natl. Acad. Sci. U S A,* **2009**, *106*, 13775-13779.

[19] Cormier, A.; Knossow, M.; Wang, C.; Gigant, B. The binding of vinca domain agents to tubulin: structural and biochemical studies. *Methods Cell Biol.,* **2010**, *95*, 373-390.

[20] Gigant, B.; Wang, C.; Ravelli, R.B.; Roussi, F.; Steinmetz, M.O.; Curmi, P.A.; Sobel, A.; Knossow, M. Structural basis for the regulation of tubulin by vinblastine. *Nature,* **2005**, *435*, 519-522.

[21] Wang, C.; Cormier, A.; Gigant, B.; Knossow, M. Insight into the GTPase activity of tubulin from complexes with stathmin-like domains. *Biochemistry,* **2007**, *46*, 10595-10602.

[22] Himes, R.H. Interactions of the *Catharanthus* (*Vinca*) alkaloids with tubulin and microtubules. *Pharmacol. Ther.,* **1991**, *51*, 257-267.

[23] Barbier, P.; Dorleans, A.; Devred, F.; Sanz, L.; Allegro, D.; Alfonso, C.; Knossow, M.; Peyrot, V.; Andreu, J.M. Stathmin and interfacial microtubule inhibitors recognize a naturally curved conformation of tubulin dimers. *J. Biol. Chem.,* **2010**, *285*, 31672-31681.

[24] Fahy, J.; Duflos, A.; Ribet, J.-P.; Jacquesy, J.-C.; Berrier, C.; Jouannetaud, M.-P.; Zunino, F. Vinca alkaloids in superacidic media: a method for creating a new family of antitumor derivatives. *J. Am. Chem. Soc.,* **1997**, *119*, 8576-8577.

[25] Lobert, S.; Vulevic, B.; Correia, J.J. Interaction of vinca alkaloids with tubulin: a comparison of vinblastine, vincristine, and vinorelbine. *Biochemistry,* **1996**, *35*, 6806-6814.

[26] Lobert, S.; Ingram, J.W.; Hill, B.T.; Correia, J.J. A comparison of thermodynamic parameters for vinorelbine- and vinflunine-induced tubulin self-association by sedimentation velocity. *Mol. Pharmacol.,* **1998**, *53*, 908-915.

[27] Taylor, R.E.; Daly, E.M. Entropy and enthalpy in the activity of tubulin-based antimitotic agents. *Curr. Chem. Biol.,* **2009**, *3*, 47-59.

[28] Lobert, S.; Frankfurter, A.; Correia, J.J. Energetics of vinca alkaloid interactions with tubulin isotypes: implications for drug efficacy and toxicity. *Cell Motil. Cytoskeleton,* **1998**, *39*, 107-121.

[29] Ferenczy, G.G.; Keseru, G.M. Thermodynamics guided lead discovery and optimization. *Drug Discov. Today,* **2010**, *15*, 919-932.

[30] Luque, I.; Todd, M.J.; Gomez, J.; Semo, N.; Freire, E. Molecular basis of resistance to HIV-1 protease inhibition: a plausible hypothesis. *Biochemistry,* **1998**, *37*, 5791-5797.

[31] Uemura, D.; Takahashi, K.; Yamamoto, T.; Katayama, C.; Tanaka, J.; Okumura, Y.; Hirata, Y. Norhalichondrin-A - an antitumor polyether macrolide from a marine sponge. *J. Am. Chem. Soc.,* **1985**, *107*, 4796-4798.

[32] Fornier, M.N. Approved agents for metastatic breast cancer. *Semin. Oncol.,* **2011**, *38 Suppl 2*, S3-10.

[33] Bai, R.; Nguyen, T.L.; Burnett, J.C.; Atasoylu, O.; Munro, M.H.; Pettit, G.R.; Smith, A.B.; Gussio, R.; Hamel, E. Interactions of halichondrin B and eribulin with tubulin. *J. Chem. Inf. Model.,* **2011**.

[34] Luduena, R.F.; Roach, M.C.; Prasad, V.; Pettit, G.R. Interaction of halichondrin B and homohalichondrin B with bovine brain tubulin. *Biochem. Pharmacol.,* **1993**, *45*, 421-427.

[35] Jordan, M.A.; Kamath, K.; Manna, T.; Okouneva, T.; Miller, H.P.; Davis, C.; Littlefield, B.A.; Wilson, L. The primary antimitotic mechanism of action of the synthetic halichondrin E7389 is suppression of microtubule growth. *Mol. Cancer Ther.,* **2005**, *4*, 1086-1095.

[36] Gordon, J.C.; Myers, J.B.; Folta, T.; Shoja, V.; Heath, L.S.; Onufriev, A. H++: a server for estimating pKas and adding missing hydrogens to macromolecules. *Nucleic Acids Res.,* **2005**, *33*, W368-371.

[37] Cornell, W.D.; Cieplak, P.; Bayly, C.I.; Gould, I.R.; Merz, K.M.; Ferguson, D.M.; Spellmeyer, D.C.; Fox, T.; Caldwell, J.W.; Kollman, P.A. A second generation force field for the simulation of proteins, nucleic acids, and organic molecules. *J. Am. Chem. Soc.,* **1995**, *117*, 5179-5197.

[38] Bashford, D.; Karplus, M. pKa's of ionizable groups in proteins: atomic detail from a continuum electrostatic model. *Biochemistry,* **1990**, *29*, 10219-10225.

[39] Jorgensen, W.L.; Chandrasekhar, J.; Madura, J.D.; Impey, R.W.; Klein, M.L. Comparison of simple potential functions for simulating liquid water. *J. Chem. Phys,* **1983**, *79*, 926–935.

[40] Aqvist, J. Ion-water interaction potentials derived from free energy perturbation simulations. . *J. Phys. Chem.,* **1990**, *94*, 8021-8024.

[41] Hansch, C. The advent and evolution of QSAR at Pomona College. *J. Comput. Aided Mol. Des.,* **2011**, *25*, 495–507.

[42] Lill, M.A. Efficient incorporation of protein flexibility and dynamics into molecular docking simulations. *Biochemistry,* **2011**, *50*, 6157-6169.

[43] Srinivasan, J.; Cheatham, T.E.; Cieplak, P.; Kollman, P.A.; Case, D.A. Continuum solvent studies of the stability of DNA, RNA, and phosphoramidate - DNA helices. *J. Am. Chem. Soc.,* **1998**, *120*, 9401-9409.

[44] Kollman, P.A.; Massova, I.; Reyes, C.; Kuhn, B.; Huo, S.; Chong, L.; Lee, M.; Lee, T.; Duan, Y.; Wang, W.; Donini, O.; Cieplak, P.; Srinivasan, J.; Case, D.A.; Cheatham, T.E., 3rd Calculating structures and free energies of complex molecules: combining molecular mechanics and continuum models. *Acc. Chem. Res.,* **2000**, *33*, 889-897.

[45] Sitkoff, D.; Sharp, K.A.; Honig, B. Accurate calculation of hydration free-energies using macroscopic solvent models. *J. Phys. Chem.,* **1994**, *98*, 1978-1988.

[46] Onufriev, A.; Bashford, D.; Case, D.A. Modification of the generalized Born model suitable for macromolecules. *J. Phys. Chem. B,* **2000**, *104*, 3712-3720.

[47] Ferguson, P.J.; Phillips, J.R.; Selner, M.; Cass, C.E. Differential activity of vincristine and vinblastine against cultured cells. *Cancer Res.,* **1984**, *44*, 3307-3312.

[48] Ferguson, P.J.; Cass, C.E. Differential cellular retention of vincristine and vinblastine by cultured human promyelocytic leukemia HL-60/Cl cells: the basis of differential toxicity. *Cancer Res.,* **1985**, *45*, 5480-5488.

[49] Lobert, S.; Ingram, J.W.; Correia, J.J. The thermodynamics of *Vinca* alkaloid-induced tubulin spirals formation. *Biophys. Chem.,* **2007**, *126*, 50-58.

[50] Lobert, S.; Fahy, J.; Hill, B.T.; Duflos, A.; Etievant, C.; Correia, J.J. *Vinca* alkaloid-induced tubulin spiral formation correlates with cytotoxicity in the leukemic L1210 cell line. *Biochemistry,* **2000**, *39*, 12053-12062.

Received: July 31, 2011 **Revised: August 28, 2011** **Accepted: August 30, 2011**